

CT Myocardial Perfusion Imaging: Clinical Implementation

Yeon Hyeon Choe

Contents

1	Introduction.....	210
2	Patient Selection for Coronary CT Angiography Based on Pretest Probability of Coronary Artery Disease.....	210
3	MRI Perfusion and Coronary CT Angiography: Insights from the Combined Approach.....	211
4	Clinical Results for Adenosine-Stress Myocardial Perfusion CT.....	218
5	Stress CT Myocardial Perfusion Protocol.....	220
6	Patient Preparation and Contraindications of CT Myocardial Perfusion.....	220
7	Image Processing and Interpretation.....	220
8	Radiation Dose.....	221
9	Cost Effectiveness of CT Perfusion.....	221
10	Limitations and Pitfalls.....	222
11	Conclusions.....	222
	References.....	223

Abstract

Despite advances, diagnosis of coronary artery diseases with coronary CT angiography (CCTA) is still hampered by artifacts from coronary artery calcium, stents, and cardiac motion. Recent CT techniques have enabled stress myocardial perfusion assessment in patients with ischemic heart diseases. Stress perfusion CT and CCTA can provide information on coronary artery anatomy and flow-limiting stenosis. CT perfusion information enhances the diagnostic accuracy of CCTA and may help to identify lesions appropriate for coronary intervention. CT perfusion is a potential economic alternative of other functional studies currently used in the evaluation of ischemic heart diseases.

Abbreviations

CAD	Coronary artery disease
CTP	CT stress myocardial perfusion
CCTA	Coronary CT angiography
FFR	Fractional flow reserve
ICA	Invasive coronary angiography
MBF	Myocardial blood flow
MDCT	Multidetector CT
MPS	Myocardial perfusion scintigraphy or SPECT
MRP	MRI stress myocardial perfusion
MDCT	Multidetector CT
MI	Myocardial infarction
NPV	Negative predictive value
PCI	Percutaneous coronary intervention
PPV	Positive predictive value

Y. H. Choe (✉)

Department of Radiology and Cardiovascular Imaging Center,
Samsung Medical Center, Sungkyunkwan University
School of Medicine, Seoul, Korea
e-mail: yhchoe@skku.edu

1 Introduction

Recently, there have been remarkable improvements in cardiac computed tomography (CT) technologies. The use of area-detector CT scanners (256-slice and 320-slice MDCT) and 128-slice dual-source scanners has decreased radiation dose to 0.5 mSv for coronary artery imaging. A meta-analysis of nine high quality trials has defined the diagnostic characteristics of coronary CT angiography using invasive coronary angiography as the gold standard. This study found that for the detection of coronary atherosclerotic plaques coronary CT angiography had a sensitivity of 96 % (95 % CI: 93–98 %) specificity of 86 % (95 % CI: 83–89 %), positive likelihood ratio of 6.38 (95 % CI: 5.18–7.87), and negative likelihood ratio of 0.06 (95 % CI: 0.03–0.10) (Gorenoi et al. 2012). However, the image quality in cardiac MDCT is degraded in patients with tachycardia or arrhythmia. Prior studies have shown that diagnostic image quality is typically obtained in 88–100 % of coronary artery segments (Hamon et al. 2007). The causes of image degradation include cardiac and respiratory motion artifacts, misregistration artifacts, blooming artifacts from heavy calcifications and stents, streak artifacts from contrast materials, and poor contrast enhancement. Although the spatial resolution of cardiac CT is improving with the adoption of new detectors, blooming artifacts still occurs. Therefore, the diagnostic capability of CCTA in the detection of significant coronary artery disease (CAD) is suboptimal in some clinical scenarios. Furthermore, the detection of CAD alone is not enough. The physiological significance of CT-detected intermediate-stenosis lesions may not be clear; clinicians favor the use of additional functional studies (e.g., exercise tests, stress nuclear studies, and stress perfusion MR imaging) in such cases. The detection of myocardial perfusion deficits using resting-state CCTA is rarely feasible in cases with severe coronary stenosis. Since knowledge of the extent and severity of inducible myocardial ischemia is critical for selecting an effective treatment strategy for patients with suspected ischemic heart disease, it would be ideal if an imaging modality could simultaneously visualize coronary anatomy and provide information on myocardial perfusion.

Coronary flow velocity reserve and fractional flow reserve (FFR) are indices of clinical decision-making with respect to percutaneous coronary interventions (PCIs). However, FFR is influenced by conditions that affect hyperemic microvascular resistance and additionally lacks the theoretical solid foundation to be a gold standard. Invasive stenosis assessment will most likely be replaced by methods that directly measure actual perfusion, such as MRI perfusion imaging (MRP) (van de Hoef et al. 2012).

2 Patient Selection for Coronary CT Angiography Based on Pretest Probability of Coronary Artery Disease

Cardiac CT is considered appropriate in patients with low-to-intermediate pretest probability of CAD (Taylor et al. 2010). In these patients, the role of CT is to exclude significant CAD. Due to the high specificity of CCTA, negative results for CAD are generally reliable; however, CCTA may not be accurate in ruling out significant CAD in patients with intermediate stenotic lesions by CCTA.

Percutaneous coronary intervention of a functionally insignificant stenotic lesion increases the chance of an adverse event, such as stent thrombosis and restenosis, as well as subsequent repeat revascularization, myocardial infarction (MI), or death. The increased risk of adverse events in such a situation clearly exceeds the low risk associated with a hemodynamically insignificant stenosis without stent placement (Lindstaedt and Mugee 2011).

Angiography is inaccurate in assessing the functional significance of a coronary stenosis when compared with the FFR, not only in lesions with 50–70 % stenosis, but also in lesions with 70–90 % angiographic stenosis (Tonino et al. 2010). According to the FFR versus angiography in multivessel evaluation (FAME) study, in 50–70 % stenosis category, 35 % of stenoses were functionally significant ($FFR \leq 0.80$). In the 71–90 % stenosis category, 80 % were functionally significant. Therefore, the decision to revascularize a coronary artery stenosis should be guided by evidence of myocardial ischemia (Tonino et al. 2010). According to the FAME study's follow-up results (Pijls et al. 2010), in 1,005 patients with multivessel CAD, the FFR-guided group received fewer stents than the angiography-guided group (2.7 ± 1.2 vs. 1.9 ± 1.3 ; $P < 0.001$) and experienced lower 2-year mortality rates and lower rates of MI (12.9 vs. 8.4 %). For lesions deferred on the basis of $FFR > 0.80$, the rate of MI was 0.2 % after 2 years, and the rate of revascularization was 3.2 %.

The DEFER study demonstrated excellent 5-year outcomes after deferral of PCI for intermediate coronary stenoses based on an FFR-guided treatment strategy (Pijls et al. 2007). In 325 patients with an intermediate stenosis, FFR was measured just before the planned intervention. If $FFR \geq 0.75$, patients were randomly assigned to deferral ($n = 91$) or performance ($n = 90$) of PCI. The composite rate of cardiac death and acute MI was 3.3 and 7.9 %, respectively ($P = 0.21$).

Although, noninvasive cardiac stress imaging may help to determine the significance of a coronary artery lesion when there is single-vessel disease, these techniques have limitations in identifying the hemodynamic significance of

individual stenoses in patients with multivessel CAD (Lindstaedt and Muge 2011). Reported sensitivities and specificities of stress echocardiography are 53–93 % and 70–100 %, respectively, under study conditions (Fox et al. 2006). The reported sensitivity of myocardial perfusion scintigraphy (MPS) ranges 70–98 %, but specificity only reaches 40–90 % (Fox et al. 2006). Myocardial perfusion imaging with single-photon emission computed tomography (SPECT) has poor concordance with FFR and tends to underestimate or overestimate the functional importance of coronary stenosis seen with angiography in comparison with FFR in patients with multivessel disease. These findings have important consequences in using MPS to determine the optimal revascularization strategy in patients with multivessel coronary disease. Compared to FFR, MPS underestimates the number of ischemic territories in 36 % of patients with multivessel disease (Melikian et al. 2010).

Adenosine-stress MRP is an accepted noninvasive test for the detection of myocardial ischemia (Schwitter et al. 2012). However, MRP is sometimes unable to differentiate subtle ischemia from artifacts (Hamon et al. 2010). The number of slices is also limited in MRP.

Recently, computational flow analysis of coronary CT data has become available for clinical applications (Koo et al. 2011). The results were comparable to those of FFR with catheterization. However, this process takes a super-computer many hours to obtain the results, which are thus not immediately available after each CT examination. On a per-vessel basis, the accuracy, sensitivity, specificity, positive predictive value (PPV), and negative predictive value (NPV) for FFRCT were 84.3, 87.9, 82.2, 73.9, and 92.2 %, respectively, and for CCTA were 58.5, 91.4, 39.6, 46.5, and 88.9 %, respectively. The area under the receiver operator characteristics curve was 0.90 for FFRCT and 0.75 for CCTA ($P = 0.001$). The FFRCT and FFR results correlated well ($r = 0.717$, $P < 0.001$) with a slight underestimation by FFRCT (0.022 ± 0.116 , $P = 0.016$).

In patients with CT-detected CAD with an intermediate degree of stenosis, diagnostic imaging should be used to guide further treatment. In this regard, stress myocardial perfusion imaging may be useful. FFR is invasive and time-consuming, and sometimes elevated despite an apparent tight stenosis (Pijls and Sels 2012). Adenosine-stress myocardial perfusion CT (CTP) is a beneficial modality because information on myocardial perfusion status is provided in addition to coronary artery anatomical information (Figs. 1, 2, 3, 4, 5, 6, 7). Therefore, CTP may also be useful in patients with intermediate-to-high pretest probability of CAD. CTP further helps to determine hemodynamic significance of morphologically significant stenosis (Bamberg et al. 2011) (Fig. 5).

The targets of adenosine CTP can be heavily calcified lesions, coronary artery stents, or multiple lesions with moderate to severe stenosis. In patients with small branch stenosis or occlusion, it may be difficult to assess the degree of stenosis of the involved vessel segments by CCTA. However, CTP may perform better in identifying perfusion abnormalities than CCTA, providing better detection of small branch lesions (Fig. 3). Therefore, CTP provides incremental values to the diagnostic accuracy of CCTA, beyond exclusion of significant CAD; patient-specific stenosis can be assessed for lesion-specific ischemia (Koo et al. 2011). In this way, the CTP technique may expand the clinical indications for CCTA.

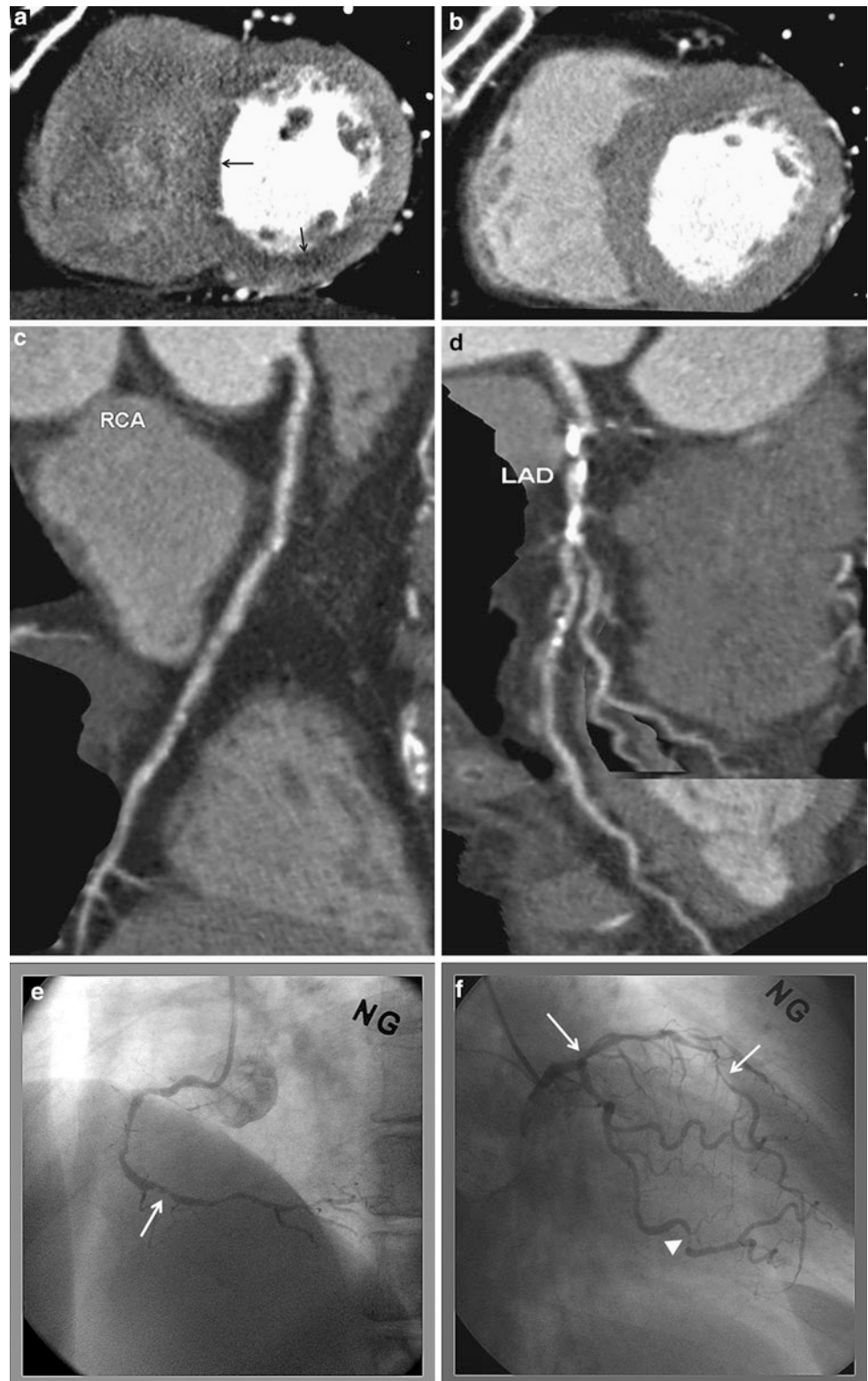
3 MRI Perfusion and Coronary CT Angiography: Insights from the Combined Approach

According to a meta-analysis (Hamon et al. 2010), the overall patient-based analysis of stress myocardial perfusion MRI demonstrated a sensitivity of 89 % (95 % CI: 88–91 %) and a specificity of 80 % (95 % CI: 78–83 %). Stress perfusion MRI is highly sensitive for detection of CAD, but its specificity remains moderate.

MR-IMPACT II study showed that the sensitivity of MRP to detect CAD was superior to SPECT, while its specificity was inferior to SPECT (Schwitter et al. 2012). For MRI and SPECT, the sensitivity scores were 67 and 59 %, respectively, while the specificity scores for MRI and SPECT were 61 and 72 %, respectively.

MRI can be used to detect flow-limiting CAD as defined by FFR, using both visual and quantitative analyses. The sensitivity and specificity of visual MRP analysis to detect stenoses at a threshold FFR of <0.75 were 82 and 94 % ($P < 0.0001$), respectively, with an area under the receiver-operator characteristic curve of 0.92 ($P < 0.0001$) (Lockie et al. 2011). In the vessels interrogated with FFR, CCTA had a sensitivity, specificity, PPV, and NPV of 93, 60, 68, and 90 %, respectively (Ko et al. 2012a). Quantitative cross-sectional parameters of the coronary lesions derived from 64-slice CCTA are significantly correlated with functional assessment by invasively determined FFR (Kristensen et al. 2010). According to a study of 42 patients, the optimal cut-off value to predict an abnormal FFR (<0.75) was 73 % for area stenosis of CCTA (sensitivity 90 %, specificity 80 %, PPV 50 %, and NPV 97 %) and 56 % for diameter stenosis of CCTA (sensitivity 80 %, specificity 67 %, PPV 35 %, and NPV 94 %), respectively (Kristensen et al. 2010). A CCTA minimal lumen diameter cut-off value of 1.2 mm had a sensitivity of 70 % and

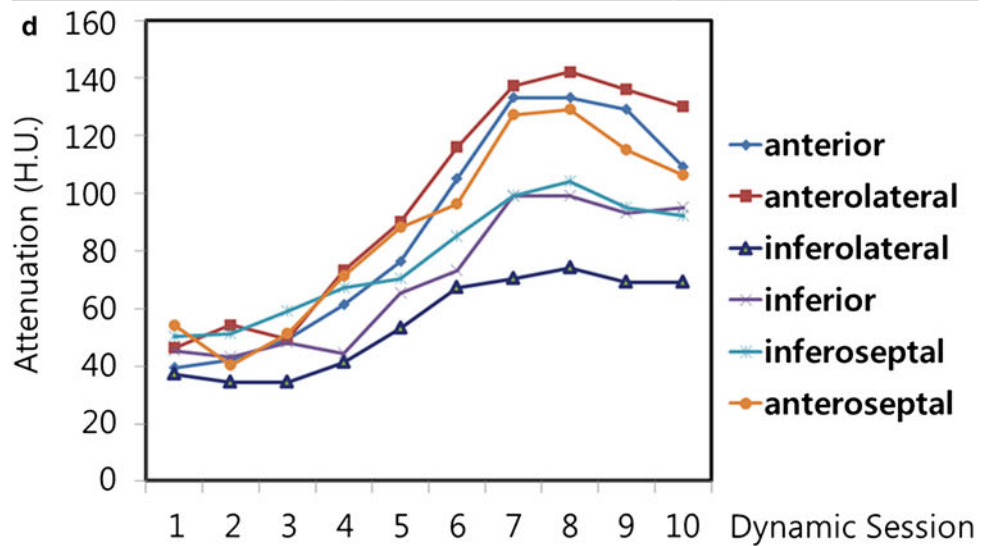
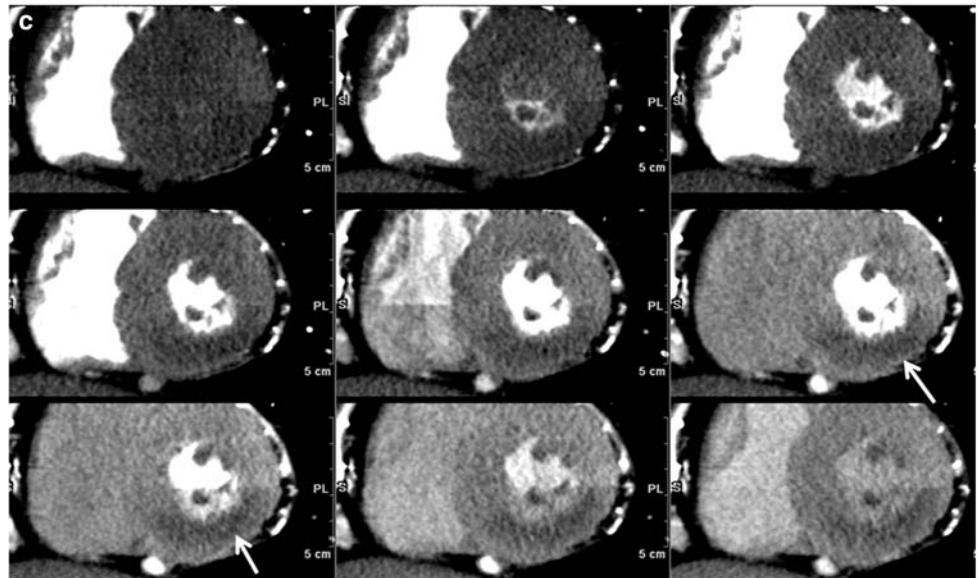
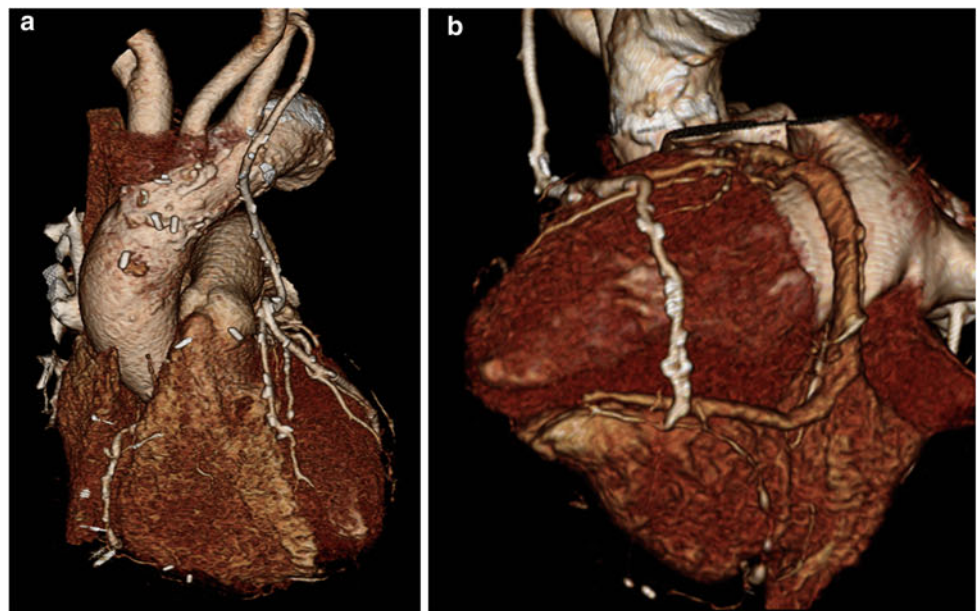
Fig. 1 A 72-year-old female with unstable angina. **a** Adenosine-stress 64-slice multidetector CT shows subendocardial perfusion defects in the septum and inferior wall (*arrows*). **b** Rest image shows no perfusion abnormalities. **c, d** Curved multiplanar reconstruction images show multiple stenoses in the right coronary artery (RCA) and calcifications in proximal-to-mid left anterior descending branch (LAD). **e, f** Catheter coronary angiography revealed focal tight stenosis in distal RCA (*arrow*), severe stenosis in proximal-to-mid LAD (*arrows*) and obtuse marginal branch (*arrowhead*)



specificity of 72 %, while a CCTA minimal lumen area cut-off value of 2 mm² had a sensitivity of 80 % and specificity of 78 %. According to a CCTA-FFR comparison study,

25.5 % (12/47) of lesions with 50–69 % stenosis severity by CCTA caused ischemia, as determined by an FFR \leq 0.80 (Koo et al. 2011).

Fig. 2 Silent ischemia in 67-year-old male with coronary bypass grafts. **a, b** Coronary bypass grafts are seen patent with good anastomosis. **c** However, stress dynamic perfusion CT shows perfusion defects (*arrows*) in inferior wall without myocardium thinning. **d** Time-attenuation curve shows significant attenuation difference between anterior and inferolateral walls of the left ventricle



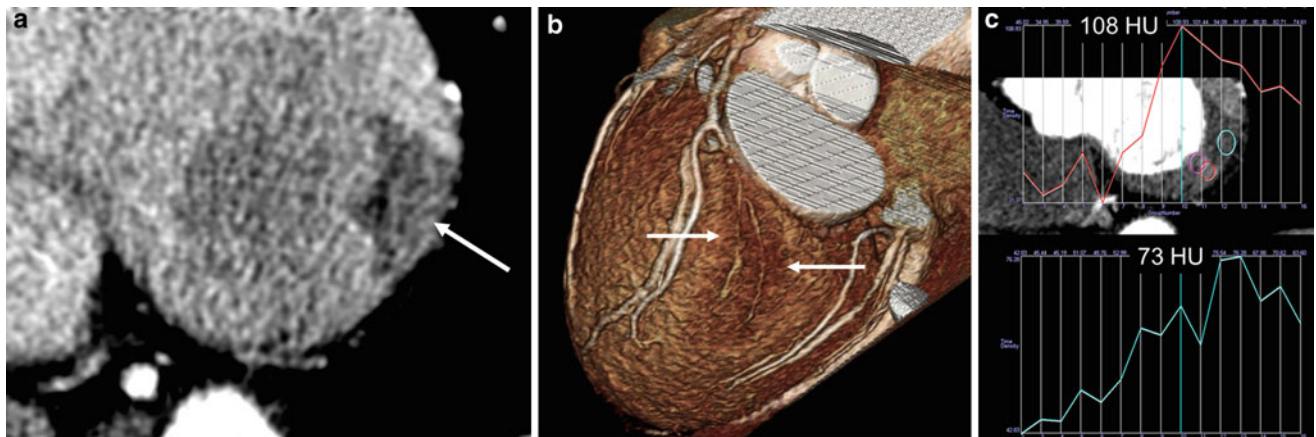


Fig. 3 Dynamic scan helps to diagnose a small branch lesion (silent ischemia in a 74-year-old male). **a** In this asymptomatic male with vascular occlusive disease, there was clearly visible myocardial ischemia in the basal inferolateral wall (*arrow*) due to occlusion of distal circumflex and obtuse marginal branches. **b** The small branch

occlusion was overlooked on CT analysis, initially. In retrospect, volume-rendered image also showed evidence of ischemia with a *darker color* (*arrows*). **c** The peak attenuation number in the perfusion defect was 73 HU and that of normal area was 108 HU

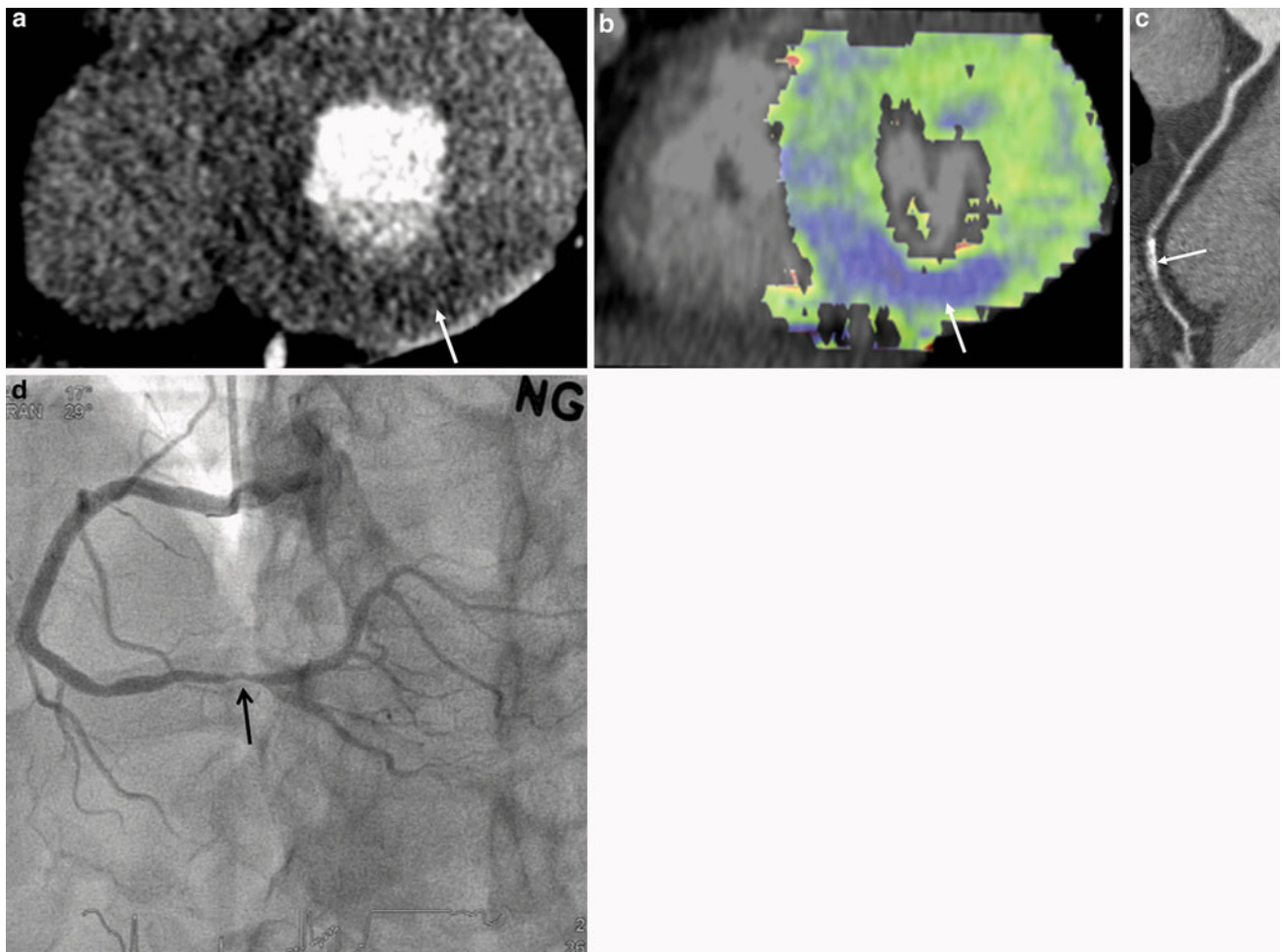


Fig. 4 A 55-year-old male with chest pain. **a, b** Short-axis reformatted stress perfusion CT (**a**) and flow map image (**b**) show decreased perfusion (*arrow*) in inferior wall. Myocardial blood flow measured $40\text{--}47 \text{ mL} \cdot 100 \text{ mg}^{-1} \text{ min}^{-1}$ in inferior wall and $86 \text{ mL} \cdot 100 \text{ mg}^{-1} \text{ min}^{-1}$ in normal myocardium.

c Curved planar reformatted image shows calcifications in the distal right coronary artery. The degree of stenosis was uncertain. **d** Catheter angiogram shows severe stenosis (*arrow*) in distal right coronary artery

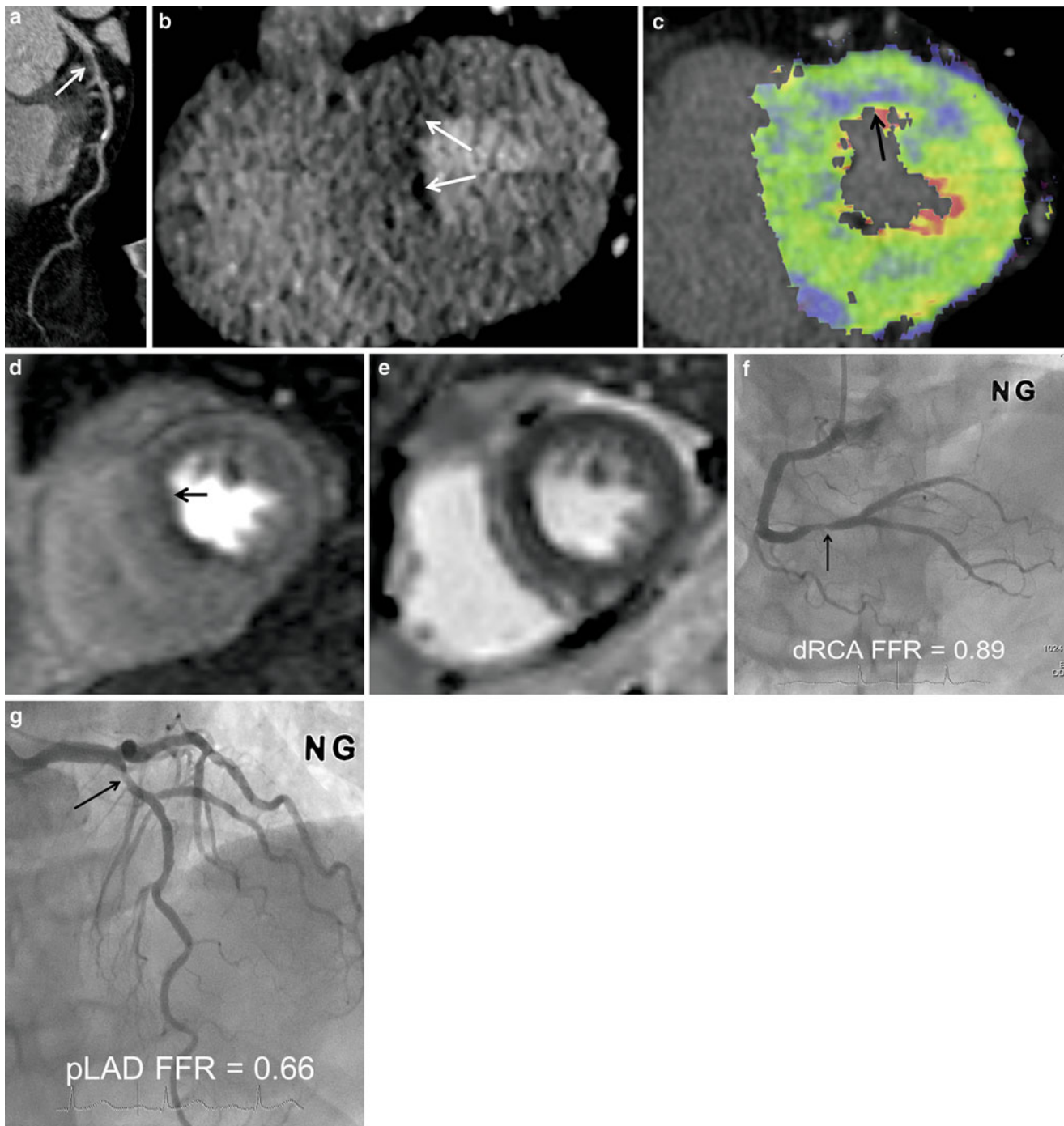


Fig. 5 A 74-year-old male with angina. **a** CT angiography shows intermediate degree stenosis (*arrow*) in the proximal left anterior descending branch (LAD) due to soft plaques. **b–e** CT perfusion reformatted images (**b**) and flow map images (**c**) show subendocardial perfusion defects (*arrows*) in anteroseptal wall. Myocardial blood flow measured $42 \text{ mL} \cdot 100 \text{ mg}^{-1} \text{ min}^{-1}$ in anteroseptal wall and

$113 \text{ mL} \cdot 100 \text{ mg}^{-1} \text{ min}^{-1}$ in normal area. Stress MR perfusion image (**d**) shows perfusion defects (*arrow*) in the same region. There was no evidence of old myocardial infarction on late gadolinium-enhanced MR images (**e**). **f, g** Adenosine fractional flow reserve was 0.89 in distal right coronary artery (**f**) and 0.66 in proximal LAD (**g**). Percutaneous coronary intervention was performed in LAD only.

According to Kirschbaum et al. (2011), MRP contributes significantly to the detection of functional significant lesions in patients with a positive CCTA. MRP and coronary flow

reserve (CFR) were performed in 50 patients with significant CAD by CCTA. MRP showed reduced perfusion in 32 patients (64%), and this finding was confirmed by CFR in

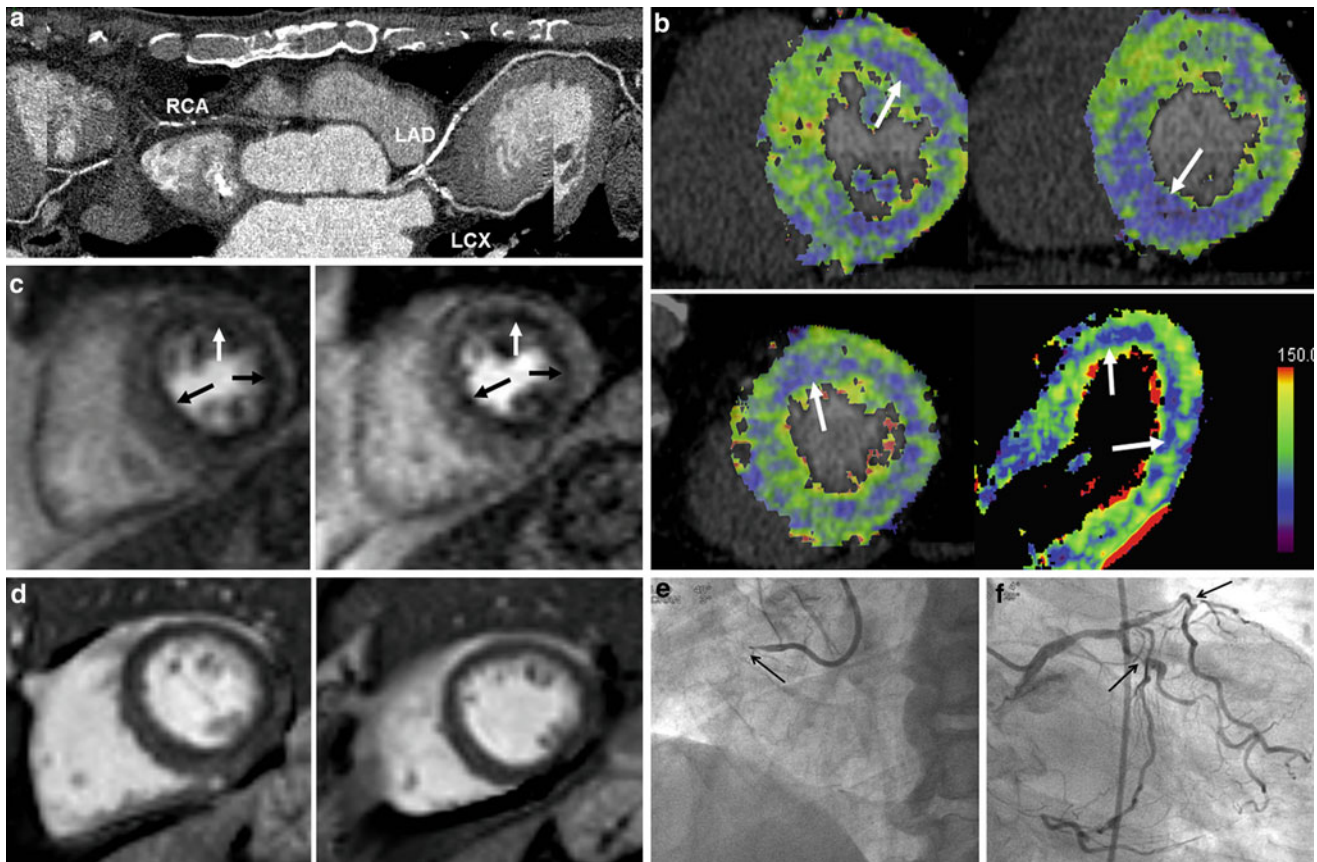


Fig. 6 Three-vessel disease with multisegment perfusion defects (70-year-old male with chest pain). **a** CT angiography shows dense calcifications in left main coronary artery, left anterior descending branch (LAD), circumflex artery (LCX), and occlusion in right coronary artery (RCA). **b** CT perfusion flow maps show decreased perfusion (*arrows*) in three-vessel territories. Myocardial blood flow measured $43\text{--}68 \text{ mL} \cdot 100 \text{ mg}^{-1} \text{ min}^{-1}$ in the areas with decreased

perfusion. **c** Stress MRI perfusion shows subendocardial perfusion defects (*arrows*) in three-vessel territories. **d** Late gadolinium-enhanced MR images show no evidence of myocardial infarction. **e, f** Catheter angiography shows occlusion of proximal right coronary artery (*arrow*) (**e**) and severe stenosis in proximal segments of left anterior descending branch and circumflex artery (*arrows*) (**f**)

27 (84 %). All 18 cases of normal MRP (36 %) were confirmed by CFR. Of the 50 patients, 20 (40 %) had multivessel disease, with MRP showing a reduced perfusion index (MPRI < 2.0) in multiple perfusion territories in 15 patients. In the remaining five patients, multivessel disease was ruled out, which was confirmed by CFR. Pretest probability of a reduced CFR in patients with a positive CCTA was 54 % (27/50). The posttest probability after MRP was 84 %. The investigators of this study proposed an algorithm with CCTA as a first-line diagnostic test followed by MRP in patients with a positive CCTA.

In a study by van Werkhoven et al. (2010), normal perfusion on MRI was observed in 33 % (5/15) of patients with significant obstructive CAD on CCTA. The majority of patients (83 %) were presented with an intermediate pretest likelihood of CAD. In all patients without significant stenosis on CCTA and normal perfusion on MRI ($n = 29$), significant stenosis was absent on invasive coronary angiography (ICA). All patients with abnormalities on both

CCTA and MRI ($n = 10$) had significant stenoses on ICA. The anatomical and functional data obtained with CCTA and MRI is complementary for the assessment of CAD. These findings support the sequential or combined assessment of anatomy and function (van Werkhoven et al. 2010).

According to Groothuis et al. (2010), the combination of both techniques enabled the clinician to evaluate both the morphology and functional relevance of CAD—comprehensively and noninvasively. Of patients without CAD on CCTA, 90.5 % (57 of 63; 95 % CI: 82.6–95.0 %) had normal myocardial perfusion on MRP. Myocardial ischemia was detected by MRP in 42.3 % (22 of 52; 95 % CI: 29.5–56 %) of patients with obstructive CAD on CCTA. Thus, CCTA can reliably rule out CAD, but detection of hemodynamically significant CAD is limited. In patients with known CAD, myocardial perfusion imaging may be more appropriate than CCTA as a first-line technique. SPECT is the modality most commonly used to assess myocardial perfusion; however, due to the increased

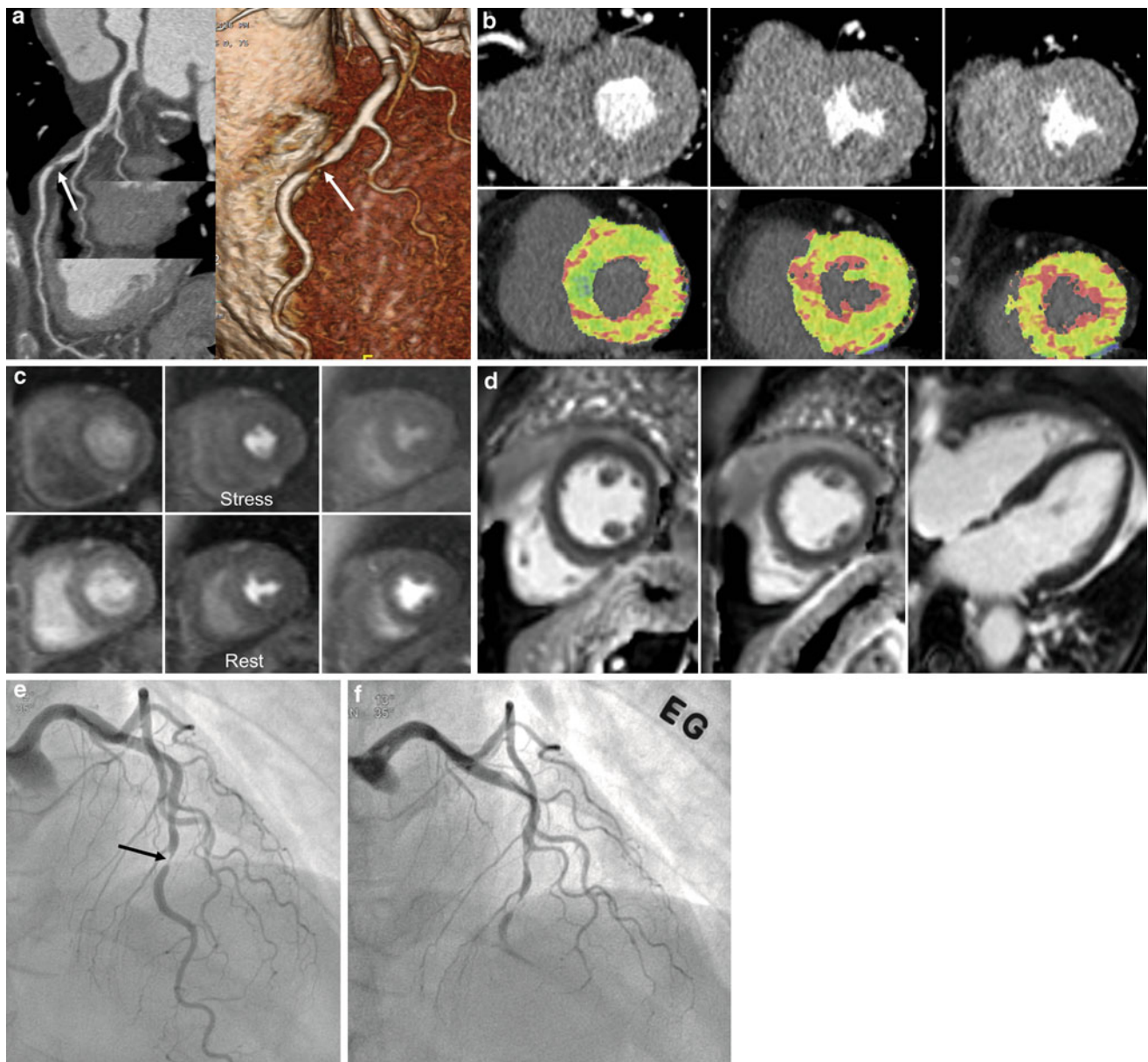


Fig. 7 A case with anatomy-physiology discrepancy (55-year-old female with chest pain). **a** CT angiography shows focal significant stenosis (*arrows*) in mid-left anterior descending branch (LAD). **b** CT perfusion reformatted and flow map images show no evidence of myocardial ischemia during stress. Myocardial blood flow measured $128 \text{ mL} \cdot 100 \text{ mg}^{-1} \text{ min}^{-1}$ overall. **c** There was no evidence of

significant perfusion defects on stress and rest perfusion MR images. **d** Late gadolinium-enhanced images show no myocardial infarcts. **e, f** Catheter angiograms show a tight stenosis (*arrow*) in mid LAD (**e**) and spasm was induced in the LAD on intraarterial ergonovine injection (**f**)

radiation burden, SPECT might not be the ideal additional functional modality used along with CCTA to evaluate patients suspected of having CAD. According to a SPECT–CCTA comparison study by Schuijff et al. (2006), of 40 patients and 62 vessels with obstructive CAD at CCTA, SPECT findings were normal in 20 patients (50 %) and 38 vessel territories (61 %).

However, according to Scheffel et al. (2010), all tested combinations of low-dose CCTA and MRP, with or without late gadolinium enhancement, were unable to improve the diagnostic performance over that of low-dose CCTA alone. Using ICA as the gold standard, low-dose CCTA outperforms MRI with regard to sensitivity and NPV, whereas MRI is more specific and has a higher PPV than low-dose CCTA.

4 Clinical Results for Adenosine-Stress Myocardial Perfusion CT

Recent literature has shown the potential advantage of MDCT for CCTA during adenosine-stress (Bamberg et al. 2012; Bastarrika et al. 2010; Bettencourt et al. 2011; Cury et al. 2011; Feuchtner et al. 2011; George et al. 2009; Ho et al. 2010; Ko et al. 2011, 2012a, b; Nagao et al. 2011; Rocha-Filho et al. 2010; Ruzsics et al. 2009; Tamarappoo et al. 2010; Wang et al. 2012; Weininger et al. 2010) (Table 1). The feasibility of adenosine-stress CT has been documented by George et al. (2006) in an experimental animal model. According to Rocha-Filho et al. (2010), adenosine-stress perfusion imaging (single static scan) in addition to 64-slice dual-source CCTA demonstrated improved sensitivity, specificity, PPV, and NPV of CCTA for CAD diagnosis (83–91, 71–91, 66–86, and 87–93 %, respectively).

Feuchtner et al. (2011) used high-pitch stress perfusion CT (single scan) in 39 patients, yielding a per-vessel sensitivity of 96 % with 88 % specificity, 93 % PPV, and 94 % NPV in the detection of perfusion defects in comparison with cardiac MRI; the per segment sensitivity was 78 % with 87 % specificity, 83 % PPV, and 84 % NPV. In 25 patients with CAD, confirmed by ICA, the addition of CTP to CCTA improved accuracy from 84 to 95 % for the detection of stenosis >70 %.

Coronary CT angiography during adenosine infusion is possible with the use of an area-detector CT (256- or 320-slice CT). Ko et al. (2012a) compared CTP with FFR in 42 patients using a 320-detector row CT scanner and prospective electrocardiography (ECG)-gating for the detection of stenosis >50 %. FFR ≤ 0.8 was considered as an indication of significant ischemia. CTP imaging correctly identified 31 of 41 (76 %) ischemic territories and 38 of 45 (84 %) non-ischemic territories. Per-vessel territory sensitivity, specificity, PPV, and NPV of CTP were 76, 84, 82, and 79 %, respectively. The combination of ≥50 % stenosis on CTA and a perfusion defect on CTP was 98 % specific for ischemia, while the presence of <50 % stenosis on CTA and normal perfusion on CTP was 100 % specific for exclusion of ischemia. Mean radiation for CTP and combined CT was 5.3 and 11.3 mSv, respectively.

Contemporary MDCT techniques enable dynamic acquisition of image data during adenosine-stress administration. According to Bamberg et al. (2010), data are acquired, alternating between two table positions, covering 73 mm during systolic phases for 30 s using 100 kVp. Radiation dose was 2.3 mSv for CCTA and 9.6 mSv for dynamic scanning. Ho et al. (2010) used this technique for myocardial perfusion imaging in 35 patients. There was a 1.5-fold difference between stress and rest myocardial blood

flow (MBF) in normal tissue. In reversible defects, MBF was 0.65 ± 0.21 mL/mL/min and 0.63 ± 0.18 mL/mL/min at stress and rest, respectively. In comparison with nuclear myocardial perfusion imaging, the sensitivity, specificity, PPV, and NPV of CTP for identifying segments with perfusion defects was 83, 78, 79, and 82 %, respectively. The sensitivity, specificity, PPV, and NPV of CTP compared with ICA were 95, 65, 78, and 79 %, respectively.

According to Bamberg et al. (2011), the diagnostic accuracy of CCTA was low for the detection of hemodynamically significant stenosis (PPV per coronary segment, 49 %; 95 % CI: 36–60 %). With the use of estimated MBF to reclassify lesions depicted with CT angiography, 30 of 70 (43 %) coronary lesions were graded as hemodynamically insignificant, which significantly increased PPV to 78 % (95 % CI: 61–89 %; $P = 0.02$). The presence of a coronary artery stenosis with a corresponding MBF less than 75 mL/100 mL/min had a high risk for hemodynamic significance (odds ratio, 86.9; 95 % CI: 17.6–430.4). In a pig model, in the ischemia group, MBF under stress was 74.0 ± 21.9 mL/100 mL/min in the post-stenotic myocardium and 117.4 ± 18.6 mL/100 mL/min in the remaining normal myocardium ($P = 0.0024$) (Mahnken et al. 2010). CTP is moderately accurate in identifying ischemia as assessed by FFR in patients considered for revascularization, while CCTA/CTP is highly accurate in the detection and exclusion of ischemia in territories where CCTA and CTP are concordant.

The results of Weininger et al. (2010) suggested the clinical feasibility of CTP in patients with acute chest pain. Compared to MRI and SPECT, dynamic real-time perfusion CT and first-pass dual-energy perfusion CT showed good agreement for the detection of myocardial perfusion defects.

Myocardial blood flow measured by CTP may predict functional recovery of the left ventricle after coronary bypass graft surgery (CABG) (Shikata et al. 2010). In a study on 19 patients who underwent CABG, MBF in revascularized areas increased significantly (pre-CABG 1.18 ± 0.45 mL · g⁻¹ · min⁻¹, post-CABG 1.99 ± 0.66 mL · g⁻¹ · min⁻¹, $P < 0.001$), whereas nonischemic areas showed no significant difference (1.79 ± 0.70 and 1.97 ± 0.46 mL · g⁻¹ · min⁻¹, $P = 0.14$).

CTP may provide information on MI (Nakauchi et al. 2012) with better sensitivity than rest imaging. However, CTP has limitations in the detection of nonviable myocardial segments. Late or delayed CT at 7–10 min after injection of 100–120 mL of contrast material may help to detect nonviable hyperenhancing lesions of MI on the addition of radiation (Choe et al. 2008). Fat infiltration in the infarct may suggest the diagnosis of old MI without providing information on the depth of myocardial fibrosis. A profoundly low MBF value of dynamic CTP suggests the diagnosis of nonviable myocardium. The cutoff value may be around

Table 1 Diagnostic accuracy and radiation dose of combined coronary CT angiography and CT perfusion according to each scan protocol in the diagnosis of significant coronary artery stenosis with myocardial ischemia

Authors/year	Number of patients	Scanner type	Reference standard	Protocol	Diagnostic parameters (added value with CTP)			Radiation dose (mSV)			
					Sensitivity (%)	Specificity (%)	PPV (%)	NPV (%)	CTP	CCTA Total	
Bamberg et al. 2011	33	128 ds	ICA ($\geq 50\%$) FFR (≤ 0.75)	P-CCTA,	91	69	79	85	10.0	3.1	13.1
				D-CTP	93 (-7)	87 (36)	75 (28)	96.7 (-3.3)			
Wang et al. 2012	30	128 ds	ICA ($\geq 50\%$) SPECT	P-CCTA,	90 (0)	81 (30)	58 (23)	97 (2)	11.5	4.0	15.5
				D-CTP	85	92	55	98			
Feuchner et al. 2011	39	128 ds	ICA ($\geq 70\%$) (n = 25) MRI (1.5T) (n = 30)	H-CTP, H- or	100 (2)	74 (47)	97 (13)	100 (20)	1.1	1.9	3.0
				P-CCTA	78	88	83	84			
Ko et al. 2012a	42	320 ss	FFR (≤ 0.8)	P-CTP, delay P-CCTA, rest P-CCTA	68 (-25)	98 (38)	97 (29)	77 (-23)	6.4	5.8	13.7
Blankstein et al. 2009	34	64 ds	ICA ($\geq 50\%$), SPECT ICA ($\geq 70\%$), SPECT	R-CTP,	79	80	73	84	9.5	2.0	12.7
				P-CCTA, delay P-CCTA	86	68	42	95			
Rocha-Filho et al. 2010	35	64 ds	ICA ($\geq 50\%$) ICA ($\geq 70\%$)	R-CTP,	91 (8)	91 (20)	86 (20)	93 (6)	9.8	2.0	11.8
				P-CCTA	91 (9)	78 (14)	53 (15)	97 (4)			
Bettencourt et al. 2011	90	64 ss	ICA ($\geq 50\%$) ICA ($\geq 70\%$)	R-CTP,	61 (-30)	97 (17)	87 (27)	88 (-8)	4.1	1.0	6.8
				P-CCTA	69 (-28)	96 (15)	78 (26)	94 (-5)			
Ko et al. 2011	41	64 ds	ICA ($\geq 50\%$) (n = 41) MRI (1.5T) (n = 28)	R-CCTA, R-E	89	76	81	86	5.8	8.6	14.4
					89	78	74	91			
Ko et al. 2012b	45	64 ds	ICA ($\geq 50\%$)	R-CCTA, R-E	93.2 (1.4)	85.5 (17.8)	88.3 (14.7)	91.4 (3.9)	5.7	10.8	16.5

Note CCTA = coronary CT angiography, CTP = stress CT perfusion, D = dynamic scan, ds = dual-source, E = dual energy, FFR = fractional flow reserve, H = high-pitch, ICA = invasive coronary angiography, NPV = negative predictive value, P = prospective, PPV = positive predictive value, R = retrospective helical, S = static or single scan, SPECT = single-photon emission tomography, ss = single source

Diagnostic accuracy was based on per segment (comparison with MRI or SPECT) or per-vessel territory (comparison with ICA or FFR)

Radiation dose was described or corrected with conversion factor of 0.017 for the calculation of effective radiation dose in all studies

Total dose refers to the sum of the radiation doses of all CT scans including calcium score and late CT scan according to the protocol in each study

50 mL · 100 mg⁻¹ min⁻¹. Fixed perfusion defects on stress and rest images are highly suggestive of MI.

Recent technology enables dual-energy application in cardiac imaging, although cardiac motion artifacts are still barriers in obtaining appropriate information on iodine distribution in ischemic myocardium. Dual-energy CT has demonstrated effective visualization of resting ischemia (Ruzsics et al. 2009). However, further research is necessary to validate the usefulness of dual-energy CT for the assessment of myocardial ischemia at rest and under stress.

5 Stress CT Myocardial Perfusion Protocol

A typical example of stress CT myocardial perfusion protocol is as follows (Fig. 8):

- Precontrast calcium scoring.
- Test bolus technique or bolus-tracking technique for timing of stress CT, unless using a fixed delay time of 4–6 s before the start of image acquisition after commencement of contrast injection.
- Adenosine infusion.
- Stress CT (single-phase or dynamic multiphase).
- Coronary CT angiography.
- Late CT (optional, 6–10 min delay).

The whole examination requires 25–30 min in our institution, if operated by skillful and experienced technologists. Adoption of a dynamic rest perfusion CT may not be recommended because of additional radiation.

6 Patient Preparation and Contraindications of CT Myocardial Perfusion

Stressors such as dipyridamole and adenosine have been used in the field of nuclear cardiac imaging. Dipyridamole blocks adenosine reuptake. Adenosine dilates coronary arteries by interaction with adenosine-A₂ receptor. The direct infusion of adenosine at the dose of 140 · μg · kg⁻¹ min⁻¹ using an infusion pump increases coronary flow velocity 4.4-fold (Verani 2000). Image acquisition begins 3–6 min after initiation of adenosine infusion. The plasma half-life of adenosine is 2–10 s. Regadenoson is an adenosine A (2A) receptor agonist approved for use as a pharmacologic stress agent for radionuclide myocardial perfusion imaging in patients unable to undergo adequate exercise stress. Regadenoson is easy to dose in a 10 s bolus and appears to be generally well tolerated, with most adverse events beginning soon after administration and resolving within approximately 15 min. No unexpected treatment-emergent ECG changes occurred with regadenoson in phase III trials (Garnock-Jones and Curran 2010).

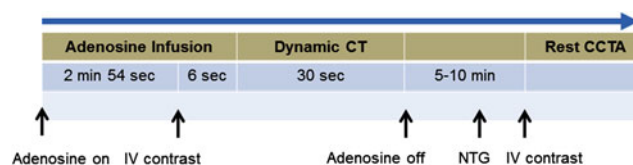


Fig. 8 A diagram of the CT perfusion protocol using a dynamic stress CT technique. CCTA coronary CT angiography, IV intravenous, NTG nitroglycerin

Patients must refrain from coffee, tea, chocolate, or any other source of caffeine for at least 24 h before the examination. Dipyridamole is discontinued for 24 h before CTP.

Contraindications of adenosine include:

- Asthma or active bronchospasm.
- Severe chronic obstructive pulmonary disease with rest hypoxia.
- Recent use of theophylline/caffeine.
- Advanced atrioventricular block.
- Severe hypotension.
- Sick sinus syndrome.
- Very early (within 2 days) after acute MI or unstable angina.

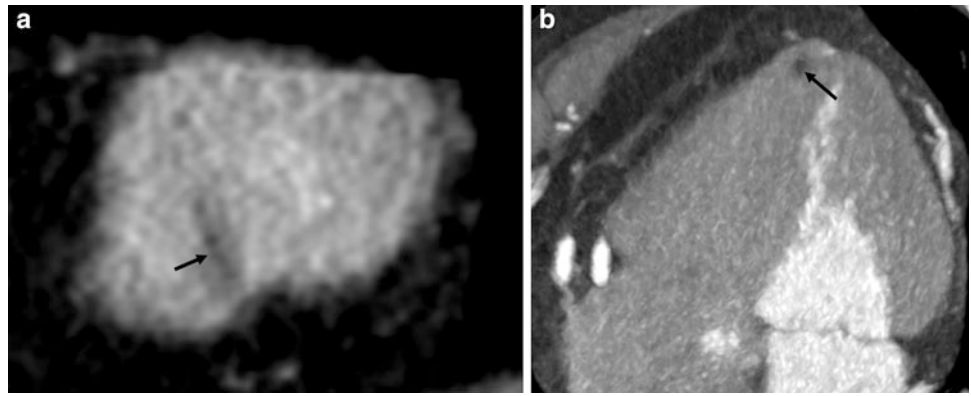
Adenosine is remarkably safe; while side effects occur in 80 % of patients with atrioventricular block in 8 % and ST-T change in 6 % (Verani 2000). Side effects resolve within 1–2 min after test completion. In case of severe reaction, 100 mg theophylline (aminophylline), an antagonist, is slowly injected intravenously and repeated for 2–3 min with a maximum dose of 300 mg.

It is advisable to monitor blood pressure, arterial oxygen level (pulse oxymeter), and ECG for myocardial ischemia and atrioventricular block during adenosine infusion. Three extremities are used. Intravenous routes are secured for adenosine infusion and contrast injection in each arm, respectively, and blood pressure is monitored in a lower extremity (calf). In the case of severe bradycardia associated with excessive adenosine infusion, aborting the dynamic CT scan should be considered.

7 Image Processing and Interpretation

The MMWP workstation (Siemens Medical Solutions, Erlangen, Germany) with Syngo VPCT body-myocardium (software) is one example of a commercial solution for image processing of dynamic perfusion data. Motion correction is performed after selecting a baseline image among those of the dynamic series; the more motion artifacts there are, the more myocardium that is lost. Then, myocardial segmentation is performed. The whole volume of the myocardium is included in the region-of-interest (ROI) for the segmentation process. Aortic attenuation is measured

Fig. 9 A pitfall in image interpretation. **a** A focal area of nonspecific fat in apical myocardium mimics a perfusion defect on dynamic CT perfusion (*arrow*). **b** CT angiography image shows an area of fat (*arrow*) in the cardiac apex



for the calculation of the arterial input function. ROIs should be placed in the regions of normal and abnormal myocardium for the flow map analysis.

One should be careful when interpreting CTP in patients with significant motion artifacts, beam-hardening artifacts, anatomic variation, and nonspecific fat infiltration in the myocardium (Figs. 9, 10). Keep in mind that the basal interventricular septum and the mid-to-basal posterolateral wall show variable degrees of low attenuation or low MBF in normal subjects. Minimum intensity projection (MinIP) images with 3 mm thickness and diastolic images are better for depicting perfusion defects on reconstructed CT images (Ghoshhajra et al. 2011).

8 Radiation Dose

Recent CT techniques enable low-dose dynamic or static CTP. Adoption of automated dose modulation of X-ray tube current (and more recently, voltage) reduces the radiation dose received by patients during CT examination. In addition, iterative reconstruction methods permit further reductions of radiation dose. Currently, CTP delivers 1 mSv with low-dose high-pitch scanning, 10 mSv with dynamic scanning using a 128-slice dual-source CT scanner, and 5 mSv with a 320-slice area-detector CT, in addition to the dose associated with CCTA (Bamberg et al. 2010; Feuchtner et al. 2011; Ko et al. 2012a). Generally, static techniques for CTP deliver radiation doses to patients similar to those of CCTA.

Our results of dynamic CT perfusion from 330 consecutive patients showed maximum attenuation difference between normal and abnormal myocardium occurred at 12.0–24.3 s after initiation of contrast injection. The mean radiation dose of a dynamic stress scan was 12.1 ± 1.6 mSv (range, 9.2–16.4 mSv) with fixed tube current at 100 kVp, 7.7 ± 2.5 mSv (range, 3.3–16.1 mSv) with automatic tube current modulation, and 3.8 ± 1.3 mSv (range, 2.0–7.6 mSv) with automatic tube current modulation and half-duration (14 s) scan.

9 Cost Effectiveness of CT Perfusion

Between 20 and 25 % of patients can avoid invasive testing by undergoing functional testing as a gateway to angiography without substantial effects on outcomes (Sharples et al. 2007). Positive functional tests were confirmed by positive angiography in 83 % of SPECT patients, 89 % of MRI patients, and 84 % of stress echocardiography patients. In a randomized trial of 898 patients, negative functional tests were followed by positive angiograms in 31 % of SPECT patients, 52 % of MRI patients, and 48 % of stress echocardiography patients tested (Sharples et al. 2007).

Sixty-four-slice CT appears to be as good as, but cheaper than MPS for the diagnosis of CAD. Consequently, 64-slice CT is likely to be a cost-effective replacement for MPS in diagnosing CAD (Mowatt et al. 2008). Diagnostic strategies involving 64-slice CT seem to still require ICA for CT false-positives in terms of quantifying the degree of stenosis. Due to non-diagnostic CT images, approximately 3.6 % of the examined patients required a subsequent ICA (Gorenai et al. 2012). The high specificity of 64-slice CT avoids the costs of unnecessary ICA in those who do not have CAD. The health-economics model using ICA as the reference standard showed that at a pretest probability for CAD of 50 % or lower, CCTA resulted in lower cost per patient with true positive diagnosis. At a pretest probability of CAD of 70 % or higher, ICA was associated with lower cost per patient with true positive diagnosis (Gorenai et al. 2012). There is a trend of declining diagnostic cardiac catheterization, while the ratio of PCI over catheterization is increasing (Jones et al. 2011).

Using intracoronary pressure measurement as the reference standard, CCTA compared with ICA had a sensitivity of 80 % (95 % CI: 61–92 %) versus 67 % (95 % CI: 51–78 %), a specificity of 67 % (95 % CI: 47–83 %) versus 75 % (95 % CI: 60–86 %), an average positive likelihood ratio of 2.3 versus 2.6, and an average negative likelihood ratio of 0.3 versus 0.4, respectively (Gorenai et al. 2012). From both a medical and a health-economics perspective,

Fig. 10 Beam-hardening artifact. A band-like dark area (arrow) is due to beam-hardening artifacts from the highly attenuated descending thoracic aorta on a dynamic CT reformatted image (a) and color map image (b). Window width and level of the reformatted images were 229 and 77, respectively

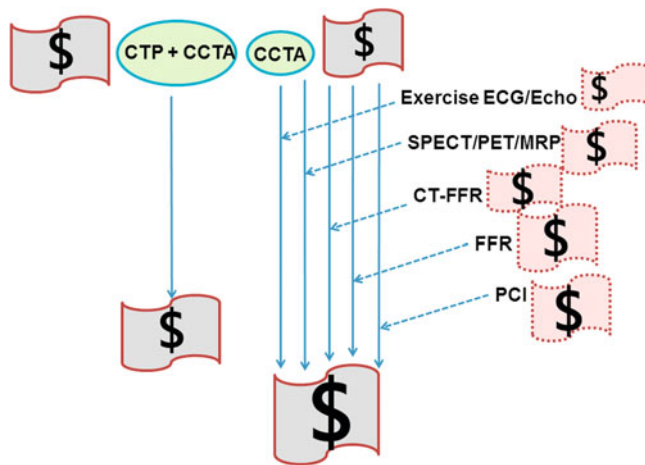
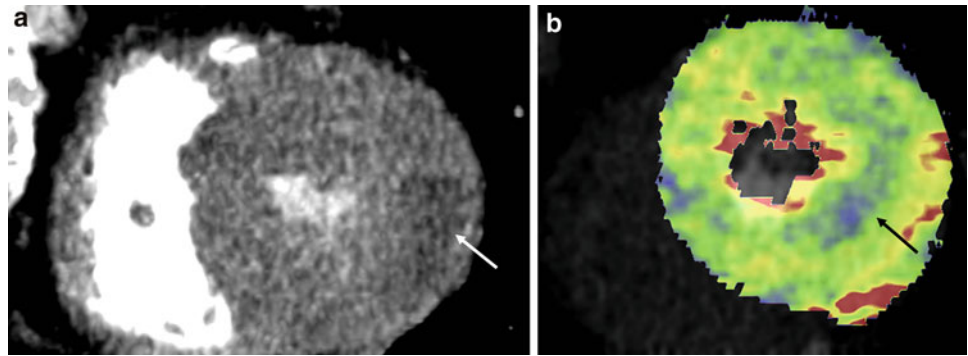


Fig. 11 A chart showing economic consideration using CT perfusion (CTP) and coronary CT angiography (CCTA) together. Expenses of an additional examination or examinations including exercise electrocardiography (ECG), exercise echocardiography (Echo), single-photon emission tomography (SPECT), positron emission tomography (PET), MRI perfusion (MRP), CT-fractional flow reserve (CT-FFR), FFR, and percutaneous coronary intervention (PCI) can be saved, if CTP and CCTA are performed together as a one-stop examination and provide relevant information on coronary artery disease

neither CCTA nor ICA may be recommended as the single diagnostic test for identifying or ruling out functionally relevant coronary stenoses (Gorenoi et al. 2012).

CTP (A) takes longer time than CCTA. It requires more personnel and it delivers a greater radiation and contrast material burden. However, its value may be equivalent to that of a combination of CCTA (B) with SPECT/PET or adenosine-stress perfusion MR imaging (C). Savings will be defined as the cost difference ($B + A - C$) (Fig. 11). Suppose that we have a patient with chest pain due to intermediate degree stenotic lesions in three vessels. If we can omit FFR (D) during catheterization because of having obtained information on coronary flow physiology, additional money can be saved. If we can differentiate hemodynamically significant lesions and not perform PCI on all intermediate lesions, we can achieve further savings (E). If CTP replaces diagnostic ICA (F), we can save money

($F - A$). If CTP replaces CT FFR (G), again, we can save money ($G + B - A$). An economic evaluation of CTP versus CCTA for health outcomes and costs should be performed in the future.

10 Limitations and Pitfalls

Current dynamic CT technology has limitations in anatomic coverage (7 cm) with a second generation dual-source CT. Beam-hardening artifacts are problematic for the interpretation of CT images. However, an algorithmic approach may solve this problem (Kitagawa et al. 2010). Relative low tissue contrast of CT may decrease the sensitivity of CTP. However, a MBF map obtained from CT data provides important information on myocardial perfusion.

Another limitation of the dual-source dynamic CTP protocol is the limited temporal resolution, as datasets are only acquired every two or four heartbeats. This limitation could result in an underestimation of blood flow, particularly during stress as temporal resolution requirements for MBF quantification become more critical with increasing MBF.

On the other hand, higher spatial resolution of CT compared with MRI may eliminate errors associated with dark-rim artifacts on MRP. The availability of CTP is still limited, because it is a new technique. Widespread use of CTP should be preceded by the results of basic and clinical research, with further education of radiologists, technologists, and clinicians.

Randomized trials will be needed to compare the clinical effectiveness of the CCTA/CTP examination with other modalities (Blankstein and Jerosch-Herold 2010). The prognostic value of CTP is not known and should be evaluated in the future.

11 Conclusions

Stress perfusion CTP and CCTA can provide information on coronary artery anatomy and physiology simultaneously. Wide-coverage (dual-source) CT scanners with prospective

ECG-gated scanning techniques permit low-radiation, dynamic imaging of the myocardium after contrast injection. CTP is expected to play some role in the evaluation of ischemic heart disease with coronary arteries that display an intermediate-to-high degree of stenosis for patients with intermediate-to-high pretest probability of CAD.

References

- Bamberg F, Klotz E, Flohr T, Becker A, Becker CR, Schmidt B, Wintersperger BJ, Reiser MF, Nikolaou K (2010) Dynamic myocardial stress perfusion imaging using fast dual-source CT with alternating table positions: initial experience. *Eur Radiol* 20:1168–1173. doi:10.1007/s00330-010-1715-9
- Bamberg F, Becker A, Schwarz F, Marcus RP, Greif M, von Ziegler F, Blankstein R, Hoffmann U, Sommer WH, Hoffmann VS, Johnson TR, Becker HC, Wintersperger BJ, Reiser MF, Nikolaou K (2011) Detection of hemodynamically significant coronary artery stenosis: incremental diagnostic value of dynamic CT-based myocardial perfusion imaging. *Radiology* 260:689–698. doi:10.1148/radiol.11110638
- Bamberg F, Hinkel R, Schwarz F, Sandner TA, Baloch E, Marcus R, Becker A, Kupatt C, Wintersperger BJ, Johnson TR, Theisen D, Klotz E, Reiser MF, Nikolaou K (2012) Accuracy of dynamic computed tomography adenosine stress myocardial perfusion imaging in estimating myocardial blood flow at various degrees of coronary artery stenosis using a porcine animal model. *Invest Radiol* 47:71–77. doi:10.1097/RLI.0b013e31823fd42b
- Bastarrika G, Ramos-Duran L, Rosenblum MA, Kang DK, Rowe GW, Schoepf UJ (2010) Adenosine-stress dynamic myocardial CT perfusion imaging: initial clinical experience. *Invest Radiol* 45:306–313. doi:10.1097/RLI.0b013e3181dfa2f2
- Bettencourt N, Rocha J, Ferreira N, Pires-Morais G, Carvalho M, Leite D, Melica B, Santos L, Rodrigues A, Braga P, Teixeira M, Simoes L, Leite-Moreira A, Cardoso S, Nagel E, Gama V (2011) Incremental value of an integrated adenosine stress-rest MDCT perfusion protocol for detection of obstructive coronary artery disease. *J Cardiovasc Comput Tomogr* 5:392–405. doi:10.1016/j.jcct.2011.10.002
- Blankstein R, Shturman LD, Rogers IS, Rocha-Filho JA, Okada DR, Sarwar A, Soni AV, Bezerra H, Ghoshhajra BB, Petranovic M, Loureiro R, Feuchtner G, Gewirtz H, Hoffmann U, Mamuya WS, Brady TJ, Cury RC (2009) Adenosine-induced stress myocardial perfusion imaging using dual-source cardiac computed tomography. *J Am Coll Cardiol* 54:1072–1084. doi:10.1016/j.jacc.2009.06.014
- Blankstein R, Jerosch-Herold M (2010) Stress myocardial perfusion imaging by computed tomography a dynamic road is ahead. *JACC Cardiovasc Imaging* 3:821–823. doi:10.1016/j.jcmg.2010.06.008
- Choe YH, Choo KS, Jeon ES, Gwon HC, Choi JH, Park JE (2008) Comparison of MDCT and MRI in the detection and sizing of acute and chronic myocardial infarcts. *Eur J Radiol* 66:292–299. doi:10.1016/j.ejrad.2007.06.010
- Cury RC, Magalhaes TA, Paladino AT, Shiozaki AA, Perini M, Senra T, Lemos PA, Rochitte CE (2011) Dipyridamole stress and rest transmural myocardial perfusion ratio evaluation by 64 detector-row computed tomography. *J Cardiovasc Comput Tomogr* 5:443–448. doi:10.1016/j.jcct.2011.10.012
- Feuchtner G, Goetti R, Plass A, Wieser M, Scheffel H, Wyss C, Stolzmann P, Donati O, Schnabl J, Falk V, Alkadhi H, Leschka S, Cury RC (2011) Adenosine stress high-pitch 128-slice dual-source myocardial computed tomography perfusion for imaging of reversible myocardial ischemia: comparison with magnetic resonance imaging. *Circ Cardiovasc Imaging* 4:540–549. doi:10.1161/circimaging.110.961250
- Fox K, Garcia MA, Ardissino D, Buszman P, Camici PG, Crea F, Daly C, De Backer G, Hjendahl P, Lopez-Sendon J, Marco J, Morais J, Pepper J, Sechtem U, Simoons M, Thygesen K, Priori SG, Blanc JJ, Budaj A, Camm J, Dean V, Deckers J, Dickstein K, Lekakis J, McGregor K, Metra M, Osterspey A, Tamargo J, Zamorano JL (2006) Guidelines on the management of stable angina pectoris: executive summary: the task force on the management of stable angina pectoris of the European society of cardiology. *Eur Heart J* 27:1341–1381. doi:10.1093/eurheartj/ehl001
- Garnock-Jones KP, Curran MP (2010) Regadenoson. *Am J Cardiovasc Drugs* 10:65–71. doi:10.2165/10489040-000000000-00000
- George RT, Silva C, Cordeiro MA, DiPaula A, Thompson DR, McCarthy WF, Ichihara T, Lima JA, Lardo AC (2006) Multidetector computed tomography myocardial perfusion imaging during adenosine stress. *J Am Coll Cardiol* 48:153–160. doi:10.1016/j.jacc.2006.04.014
- George RT, Arbab-Zadeh A, Miller JM, Kitagawa K, Chang HJ, Bluemke DA, Becker L, Yousuf O, Texter J, Lardo AC, Lima JA (2009) Adenosine stress 64- and 256-row detector computed tomography angiography and perfusion imaging: a pilot study evaluating the transmural extent of perfusion abnormalities to predict atherosclerosis causing myocardial ischemia. *Circ Cardiovasc Imaging* 2:174–182. doi:10.1161/CIRCIMAGING.108.813766
- Ghoshhajra BB, Rogers IS, Maurovich-Horvat P, Techasith T, Verdini D, Sidhu MS, Drzegza NK, Medina HM, Blankstein R, Brady TJ, Cury RC (2011) A comparison of reconstruction and viewing parameters on image quality and accuracy of stress myocardial CT perfusion. *J Cardiovasc Comput Tomogr* 5:459–466. doi:10.1016/j.jcct.2011.10.011
- Gorennoi V, Schonermack MP, Hagen A (2012) CT coronary angiography vs. invasive coronary angiography in CHD. *GMS Health Technol Assess* 8:Doc02. doi:10.3205/hta000100
- Groothuis JG, Beek AM, Brinckman SL, Meijerink MR, Koestner SC, Nijveldt R, Gotte MJ, Hofman MB, van Kuijk C, van Rossum AC (2010) Low to intermediate probability of coronary artery disease: comparison of coronary CT angiography with first-pass MR myocardial perfusion imaging. *Radiology* 254:384–392. doi:10.1148/radiol.09090802
- Hamon M, Fau G, Nee G, Ehtisham J, Morello R (2010) Meta-analysis of the diagnostic performance of stress perfusion cardiovascular magnetic resonance for detection of coronary artery disease. *J Cardiovasc Magn Reson* 12:29. doi:10.1186/1532-429x-12-29
- Hamon MMR, Riddell JW, Hamon M (2007) Coronary arteries: diagnostic performance of 16- versus 64-section spiral CT compared with invasive coronary angiography—meta-analysis. *Radiology* 245(3):720–731
- Ho KT, Chua KC, Klotz E, Panknin C (2010) Stress and rest dynamic myocardial perfusion imaging by evaluation of complete time-attenuation curves with dual-source CT. *JACC Cardiovasc Imaging* 3:811–820. doi:10.1016/j.jcmg.2010.05.009
- Jones WS, Patel MR, Holleran SA, Harrison JK, O'Connor CM, Phillips HR 3rd (2011) Trends in the use of diagnostic coronary angiography, percutaneous coronary intervention, and coronary artery bypass graft surgery across North Carolina. *Am Heart J* 162:932–937. doi:10.1016/j.ahj.2011.08.015
- Kirschbaum SW, Nieman K, Springeling T, Weustink AC, Ramcharitar S, Mieghem C, Rossi A, Duckers E, Serruys PW, Boersma E, de Feyter PJ, van Geuns RJ (2011) Non-invasive diagnostic workup of patients with suspected stable angina by combined computed tomography coronary angiography and magnetic resonance perfusion imaging. *Circ J* 75:1678–1684
- Kitagawa K, George RT, Arbab-Zadeh A, Lima JA, Lardo AC (2010) Characterization and correction of beam-hardening artifacts during

- dynamic volume CT assessment of myocardial perfusion. *Radiology* 256:111–118. doi:[10.1148/radiol.10091399](https://doi.org/10.1148/radiol.10091399)
- Ko BS, Cameron JD, Meredith IT, Leung M, Antonis PR, Nasis A, Crossett M, Hope SA, Lehman SJ, Troupis J, DeFrance T, Seneviratne SK (2012a) Computed tomography stress myocardial perfusion imaging in patients considered for revascularization: a comparison with fractional flow reserve. *Eur Heart J* 33:67–77. doi:[10.1093/eurheartj/ehs268](https://doi.org/10.1093/eurheartj/ehs268)
- Ko SM, Choi JW, Song MG, Shin JK, Chee HK, Chung HW, Kim DH (2011) Myocardial perfusion imaging using adenosine-induced stress dual-energy computed tomography of the heart: comparison with cardiac magnetic resonance imaging and conventional coronary angiography. *Eur Radiol* 21:26–35. doi:[10.1007/s00330-010-1897-1](https://doi.org/10.1007/s00330-010-1897-1)
- Ko SM, Choi JW, Hwang HK, Song MG, Shin JK, Chee HK (2012b) Diagnostic performance of combined noninvasive anatomic and functional assessment with dual-source CT and adenosine-induced stress dual-energy CT for detection of significant coronary stenosis. *AJR Am J Roentgenol* 198:512–520. doi:[10.2214/ajr.11.7029](https://doi.org/10.2214/ajr.11.7029)
- Koo BK, Erglis A, Doh JH, Daniels DV, Jegere S, Kim HS, Dunning A, DeFrance T, Lansky A, Leipsic J, Min JK (2011) Diagnosis of ischemia-causing coronary stenoses by noninvasive fractional flow reserve computed from coronary computed tomographic angiograms. Results from the prospective multicenter DISCOVER-FLOW (Diagnosis of Ischemia-Causing Stenoses Obtained Via Noninvasive Fractional Flow Reserve) study. *J Am Coll Cardiol* 58:1989–1997. doi:[10.1016/j.jacc.2011.06.066](https://doi.org/10.1016/j.jacc.2011.06.066)
- Kristensen TS, Engstrom T, Kelbaek H, von der Recke P, Nielsen MB, Kofoed KF (2010) Correlation between coronary computed tomographic angiography and fractional flow reserve. *Int J Cardiol* 144:200–205. doi:[10.1016/j.ijcard.2009.04.024](https://doi.org/10.1016/j.ijcard.2009.04.024)
- Lindstaedt M, Mugge A (2011) Myocardial fractional flow reserve. Its role in guiding PCI in stable coronary artery disease. *Herz* 36:410–416. doi:[10.1007/s00059-011-3486-8](https://doi.org/10.1007/s00059-011-3486-8)
- Lockie T, Ishida M, Perera D, Chiribiri A, De Silva K, Kozzerke S, Marber M, Nagel E, Rezavi R, Redwood S, Plein S (2011) High-resolution magnetic resonance myocardial perfusion imaging at 3.0-Tesla to detect hemodynamically significant coronary stenoses as determined by fractional flow reserve. *J Am Coll Cardiol* 57:70–75. doi:[10.1016/j.jacc.2010.09.019](https://doi.org/10.1016/j.jacc.2010.09.019)
- Mahnken AH, Klotz E, Pietsch H, Schmidt B, Allmendinger T, Haberland U, Kalender WA, Flohr T (2010) Quantitative whole heart stress perfusion CT imaging as noninvasive assessment of hemodynamics in coronary artery stenosis: preliminary animal experience. *Invest Radiol* 45:298–305. doi:[10.1097/RLI.0b013e3181df3cf](https://doi.org/10.1097/RLI.0b013e3181df3cf)
- Melikian N, De Bondt P, Tonino P, De Winter O, Wyffels E, Bartunek J, Heyndrickx GR, Fearon WF, Pijls NH, Wijns W, De Bruyne B (2010) Fractional flow reserve and myocardial perfusion imaging in patients with angiographic multivessel coronary artery disease. *JACC Cardiovasc Interv* 3:307–314. doi:[10.1016/j.jcin.2009.12.010](https://doi.org/10.1016/j.jcin.2009.12.010)
- Mowatt G, Cummins E, Waugh N, Walker S, Cook J, Jia X, Hillis GS, Fraser C (2008) Systematic review of the clinical effectiveness and cost-effectiveness of 64-slice or higher computed tomography angiography as an alternative to invasive coronary angiography in the investigation of coronary artery disease. *Health Technol Assess* 12:iii–iv, ix–143
- Nagao M, Kido T, Watanabe K, Saeki H, Okayama H, Kurata A, Hosokawa K, Higashino H, Mochizuki T (2011) Functional assessment of coronary artery flow using adenosine stress dual-energy CT: a preliminary study. *Int J Cardiovasc Imaging* 27:471–481. doi:[10.1007/s10554-010-9676-2](https://doi.org/10.1007/s10554-010-9676-2)
- Nakauchi Y, Iwanaga Y, Ikuta S, Kudo M, Kobuke K, Murakami T, Miyazaki S (2012) Quantitative myocardial perfusion analysis using multi-row detector CT in acute myocardial infarction. *Heart* 98:566–572. doi:[10.1136/heartjnl-2011-300915](https://doi.org/10.1136/heartjnl-2011-300915)
- Pijls NH, van Schaardenburgh P, Manoharan G, Boersma E, Bech JW, van't Veer M, Bar F, Hoorntje J, Koolen J, Wijns W, de Bruyne B (2007) Percutaneous coronary intervention of functionally nonsignificant stenosis: 5-year follow-up of the DEFER Study. *J Am Coll Cardiol* 49:2105–2111. doi:[10.1016/j.jacc.2007.01.087](https://doi.org/10.1016/j.jacc.2007.01.087)
- Pijls NH, Fearon WF, Tonino PA, Siebert U, Ikeno F, Bornschein B, van't Veer M, Klauss V, Manoharan G, Engstrom T, Oldroyd KG, Ver Lee PN, MacCarthy PA, De Bruyne B (2010) Fractional flow reserve versus angiography for guiding percutaneous coronary intervention in patients with multivessel coronary artery disease: 2-year follow-up of the FAME (Fractional Flow Reserve Versus Angiography for Multivessel Evaluation) study. *J Am Coll Cardiol* 56:177–184. doi:[10.1016/j.jacc.2010.04.012](https://doi.org/10.1016/j.jacc.2010.04.012)
- Pijls NH, Sels JW (2012) Functional measurement of coronary stenosis. *J Am Coll Cardiol* 59:1045–1057. doi:[10.1016/j.jacc.2011.09.077](https://doi.org/10.1016/j.jacc.2011.09.077)
- Rocha-Filho JA, Blankstein R, Shturman LD, Bezerra HG, Okada DR, Rogers IS, Ghoshhajra B, Hoffmann U, Feuchtner G, Mamuya WS, Brady TJ, Cury RC (2010) Incremental value of adenosine-induced stress myocardial perfusion imaging with dual-source CT at cardiac CT angiography. *Radiology* 254:410–419. doi:[10.1148/radiol.09091014](https://doi.org/10.1148/radiol.09091014)
- Ruzsics B, Schwarz F, Schoepf UJ, Lee YS, Bastarrika G, Chiaramida SA, Costello P, Zwerner PL (2009) Comparison of dual-energy computed tomography of the heart with single photon emission computed tomography for assessment of coronary artery stenosis and of the myocardial blood supply. *Am J Cardiol* 104:318–326. doi:[10.1016/j.amjcard.2009.03.051](https://doi.org/10.1016/j.amjcard.2009.03.051)
- Scheffel H, Stolzmann P, Alkadhi H, Azemaj N, Plass A, Baummueller S, Desbiolles L, Leschka S, Kozzerke S, Falk V, Boesiger P, Wyss C, Marincek B, Donati OF (2010) Low-dose CT and cardiac MR for the diagnosis of coronary artery disease: accuracy of single and combined approaches. *Int J Cardiovasc Imaging* 26:579–590. doi:[10.1007/s10554-010-9595-2](https://doi.org/10.1007/s10554-010-9595-2)
- Schuijf JD, Wijns W, Jukema JW, Atsma DE, de Roos A, Lamb HJ, Stokkel MP, Dibbets-Schneider P, Decramer I, De Bondt P, van der Wall EE, Vanhoenacker PK, Bax JJ (2006) Relationship between noninvasive coronary angiography with multi-slice computed tomography and myocardial perfusion imaging. *J Am Coll Cardiol* 48:2508–2514. doi:[10.1016/j.jacc.2006.05.080](https://doi.org/10.1016/j.jacc.2006.05.080)
- Schwiter J, Wacker CM, Wilke N, Al-Saadi N, Sauer E, Huettle K, Schonberg SO, Luchner A, Strohm O, Ahlstrom H, Dill T, Hoebel N, Simor T (2012) MR-IMPACT II: magnetic resonance imaging for myocardial perfusion assessment in coronary artery disease trial: perfusion-cardiac magnetic resonance vs. single-photon emission computed tomography for the detection of coronary artery disease: a comparative multicentre, multivendor trial. *Eur Heart J*. doi:[10.1093/eurheartj/ehs022](https://doi.org/10.1093/eurheartj/ehs022)
- Sharpley L, Hughes V, Crean A, Dyer M, Buxton M, Goldsmith K, Stone D (2007) Cost-effectiveness of functional cardiac testing in the diagnosis and management of coronary artery disease: a randomised controlled trial. *The CECaT trial*. *Health Technol Assess* 11:iii–iv, ix–115
- Shikata F, Imagawa H, Kawachi K, Kido T, Kurata A, Inoue Y, Hosokawa K, Nagao M, Higashino H, Mochizuki T, Ryugo M, Nagashima M (2010) Regional myocardial blood flow measured by stress multidetector computed tomography as a predictor of recovery of left ventricular function after coronary artery bypass grafting. *Am Heart J* 160:528–534. doi:[10.1016/j.ahj.2010.06.026](https://doi.org/10.1016/j.ahj.2010.06.026)
- Tamarappoo BK, Dey D, Nakazato R, Shmilovich H, Smith T, Cheng VY, Thomson LE, Hayes SW, Friedman JD, Germano G, Slomka PJ, Berman DS (2010) Comparison of the extent and

- severity of myocardial perfusion defects measured by CT coronary angiography and SPECT myocardial perfusion imaging. *JACC Cardiovasc Imaging* 3:1010–1019. doi:[10.1016/j.jcmg.2010.07.011](https://doi.org/10.1016/j.jcmg.2010.07.011)
- Taylor AJ, Cerqueira M, Hodgson JM, Mark D, Min J, O’Gara P, Rubin GD (2010) ACCF/SCCT/ACR/AHA/ASE/ASNC/NASCI/SCAI/SCMR 2010 Appropriate use criteria for cardiac computed tomography. A report of the American College of Cardiology Foundation Appropriate Use Criteria Task Force, the Society of Cardiovascular Computed Tomography, the American College of Radiology, the American Heart Association, the American Society of Echocardiography, the American Society of Nuclear Cardiology, the North American Society for Cardiovascular Imaging, the Society for Cardiovascular Angiography and Interventions, and the Society for Cardiovascular Magnetic Resonance. *J Cardiovasc Comput Tomogr* 4(407):e401–e433. doi:[10.1016/j.jcct.2010.11.001](https://doi.org/10.1016/j.jcct.2010.11.001)
- Tonino PA, Fearon WF, De Bruyne B, Oldroyd KG, Leesar MA, Ver Lee PN, Maccarthy PA, Van’t Veer M, Pijls NH (2010) Angiographic versus functional severity of coronary artery stenoses in the FAME study fractional flow reserve versus angiography in multivessel evaluation. *J Am Coll Cardiol* 55:2816–2821. doi:[10.1016/j.jacc.2009.11.096](https://doi.org/10.1016/j.jacc.2009.11.096)
- van de Hoef TP, Nolte F, Rolandi MC, Piek JJ, van den Wijngaard JP, Spaan JA, Siebes M (2012) Coronary pressure-flow relations as basis for the understanding of coronary physiology. *J Mol Cell Cardiol* 52:786–793. doi:[10.1016/j.yjmcc.2011.07.025](https://doi.org/10.1016/j.yjmcc.2011.07.025)
- van Werkhoven JM, Heijnenbroek MW, Schuijf JD, Jukema JW, van der Wall EE, Schreur JH, Bax JJ (2010) Combined non-invasive anatomical and functional assessment with MSCT and MRI for the detection of significant coronary artery disease in patients with an intermediate pre-test likelihood. *Heart* 96:425–431. doi:[10.1136/hrt.2009.179531](https://doi.org/10.1136/hrt.2009.179531)
- Verani M (2000) Stress approaches: techniques. In: Pohost G, O’Rourke R, Berman D, Shah P (eds) *Imaging in cardiovascular disease*, 1st edn. Lippincott Williams & Wilkins, Philadelphia, pp 151–158
- Wang Y, Qin L, Shi X, Zeng Y, Jing H, Schoepf UJ, Jin Z (2012) Adenosine-stress dynamic myocardial perfusion imaging with second-generation dual-source CT: comparison with conventional catheter coronary angiography and SPECT nuclear myocardial perfusion imaging. *AJR Am J Roentgenol* 198:521–529. doi:[10.2214/ajr.11.7830](https://doi.org/10.2214/ajr.11.7830)
- Weininger M, Schoepf UJ, Ramachandra A, Fink C, Rowe GW, Costello P, Henzler T (2010) Adenosine-stress dynamic real-time myocardial perfusion CT and adenosine-stress first-pass dual-energy myocardial perfusion CT for the assessment of acute chest pain: initial results. *Eur J Radiol*. doi:[10.1016/j.ejrad.2010.11.022](https://doi.org/10.1016/j.ejrad.2010.11.022)